Nature and Science

Websites:
http://www.sciencepub.net/nature
http://www.sciencepub.net

Emails:
naturesciencej@gmail.com
editor@sciencepub.net

MARSLAND PRESS
Multidisciplinary Academic Journal Publisher

The Role of Liver Imaging and Reporting Data System (LIRADS) Using Triphasic Computed Tomography in Diagnosis of Hepatocellular Carcinoma

Prof. Moanes Mohamed Arafa Enaba, Dr. Ahmed Abdel Hamed Mohamed, Dr. Mohamed Ibrahim Amin, Mostafa Ragaa Youssef Safa

Department of Radiodiagnosis, Faculty of Medicine, Zagazig University, Zagazig, Egypt

Abstract: The LIRADS (Liver Imaging Reporting and Data System) is an initiative sponsored by the American college of radiology which uses a standardized language & aims to categorize liver outcomes for cirrhosis patients or other risk factors for the development of HCC, allowing the radiology community to adopt standardized terminology, minimize uncertainty and errors in imaging interpretation, strengthen coordination with prescribing doctors, and promote quality assurance and research. The current version of LIRADS discusses the broad range of cirrhotic liver lesions and pseudolesions, provides a controlled imaging vocabulary lexicon, contains an ongoing illustrative atlas, provides general guidance on optimal CT and MRI procedures, review reporting, and diagnostic workup and management, and incorporates some content of non-HCC malignancies.
[Moanes Mohamed Arafa Enaba, Ahmed Abdel Hamed Mohamed, Mohamed Ibrahim Amin, Mostafa Ragaa Youssef Safa. **The Role of Liver Imaging and Reporting Data System (LIRADS) Using Triphasic Computed Tomography in Diagnosis of Hepatocellular Carcinoma.** *Nat Sci* 2020;18(11):39-57]. ISSN 1545-0740 (print); ISSN 2375-7167 (online). http://www.sciencepub.net/nature. 5. doi:10.7537/marsnsj181120.05.

Keywords: Role; Liver; Imaging; Data System; Triphasic; omography; Diagnosis; Hepatocellular Carcinoma

Introduction

The most frequent type of primary liver tumors is considered to be hepatocellular carcinoma (HCC) (ranges between 85% and 90 % of primary tumors) and after lung and stomach cancer, it is also known as the third leading cause of tumor mortality worldwide. The risk factor for hepatocellular carcinoma mainly are chronic viral hepatitis, cirrhosis, alcohol intake and hemochromatosis. Average age is 30 - 50 years and males are affected more than females[(1)].

Prognosis of HCC depends mainly on the tumor stage. Ultrasonography based monitoring programs are recommended in cirrhotic patients every 6 months. The non-invasive criteria to diagnose small HCCs in cirrhotic patients depend on evaluating the vascularity of the lesion. The techniques of choice for this step are dynamic multidetector computed tomography (MDCT) and dynamic magnetic resonance imaging (MRI). Ultrasound (US)-guided fine needle biopsy (FNB) is indicated when a diagnosis cannot be made. In lesions with atypical vascular patterns where FNB is not possible, cellular-MRI contrast agents can also play a role [(2)].

The importance of radiological enhancement pattern of the tumor has been increased in the diagnosis of HCC, recent studies by the American Association for the Study of Liver Diseases (AASLD) have shown that a tumor with a diameter of > 1 cm can be identified as a biopsy-free HCC in a cirrhotic liver with a typical dynamic study enhancement pattern (four-phase multidetector CT or enhanced contrast MRI). The tumor is characterised as having hyper-attenuation followed by hypo-attenuation (washout of the tumor in the portal venous and delayed phases) present in the arterial phase. Several researchers examined external validation of AASLD parameters, but sensitivity varied (33-81%) and small HCCs (< 3 cm) were limited to the study group[(3)].

However, imaging plays a big role in diagnosing HCC, radiologists all over the world had many problems for the definite diagnosis of HCC. Old systems only categorized the hepatic observations as positive, intermediate, negative for HCC, with a large intermediate category which includes lesions that could only be followed up without biopsy[(4)].

To solve this issue the ACR (American college of radiology) established LIRADS (Liver Imaging Reporting and Data system) in 2008 and the first online version was available in March 2011 with the help of hepatologists, hepatobiliary surgeons and pathologists. It aims to decrease the confusion in the interpretation of lesions by standardizing the content and layout of the report; improving coordination with the referring doctors; and promoting decision-making (e.g. for transplantation, ablative therapy or chemotherapy, results tracking, assurance of quality and research [(5)].

A system used to interpret and report liver computed tomography (CT) and magnetic resonance imaging (MRI) scans in patients at risk for HCC is the Liver Imaging Reporting and Data System (LI-RADS) [4].

Five categories are used in LIRADS to classify individual results as per the degree. The cornerstone imaging characteristics of imaging include: mass-like structure, hyperenhancement of the arterial phase, hypoenhancement of the portal venous phase or later phase, arise in diameter of 10 mm or more in 1 year and a tumor inside the vein's lumen. LIRADS is a developing system that continues to evolve and is expected to be updated frequently in future versions [6].

Aim of Work

The objective of this research is to assess the value of using LIRADS classification with triphasic CT scan in diagnosis of HCC.

Gross Anatomy

The liver normally occupies the upper right quadrant of the abdominal cavity just below the right hemi-diaphragm and is fixed in place by multiple ligaments. It is shielded by the lower ribs and retains its location by ligamentous attachments known as peritoneal reflections. These attachments, while not true ligaments, are vascular and are in continuity with the Glisson capsule or the liver visceral peritoneum equivalent [7].

A. Segmental anatomy:

Radiologists may accurately localize a lesion to a given segment for the surgeon, this description is of both functional and pathological importance. Each segment has its own supply of blood (arterial, portal venous and hepatic venous). The liver is subdivided into eight sections, the hepatic veins right, middle and left divide the liver longitudinally into four sections, each of which is divided horizontally by an imaginary line along the main branches of the right and left portal[8].

The caudate lobe is segment I. Segments II, III are the parts of the left lobe that are located to the left of the falciform ligament (Figure 1 & 2) [9]. The medial part of the left hepatic lobe (quadrate lobe) among the falciform ligament and the line of the vena cava-gall bladder / middle hepatic vein is segment IV. Segment IV is subdivided into subsections IVa cranial and IVb caudal in the Bismuth classification [8].

The right hepatic lobe is split into subsegments V through VIII with a clockwise numbering scheme inferomedially adjacent to the gall bladder beginning from sub-segment V (Figure 3) [9].

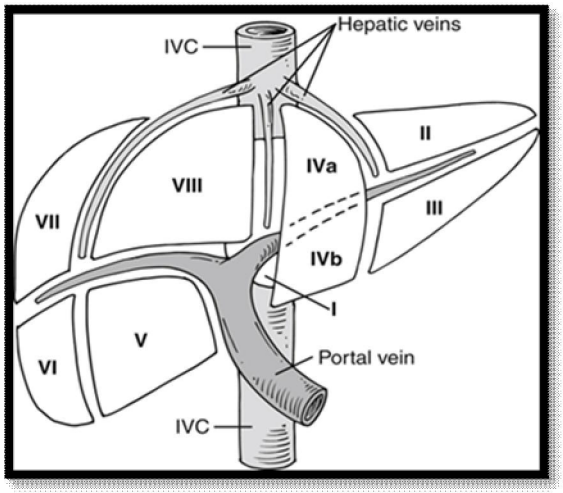

Figure 1: Diagram shows surgical segments of the liver [10]

Figure 2: Axial US image shows approach to the left hemi-liver [11]

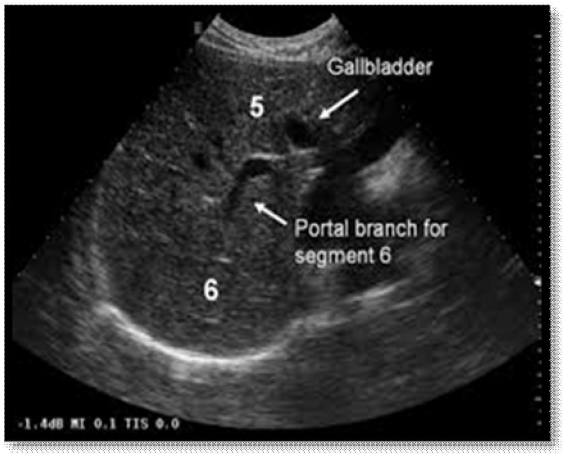

Figure 3: Axial US image shows an approach to the right hemiliver. Right liver segments can be visualized [9].

B. Vascular anatomy:

1-Hepatic arteries:

The popular hepatic artery is mostly created by the celiac trunk. Behind the pylorus, the gastroduodenal artery and the proper hepatic artery that passes to the portal vein through the anteromedial hepatoduodenal ligament and to the left of the common bile duct, courses to the right and branches into its two main branches. In liver hilum, the proper hepatic artery bifurcates into the right hepatic artery and the left hepatic artery (Table 1 & Figure 4) [12].

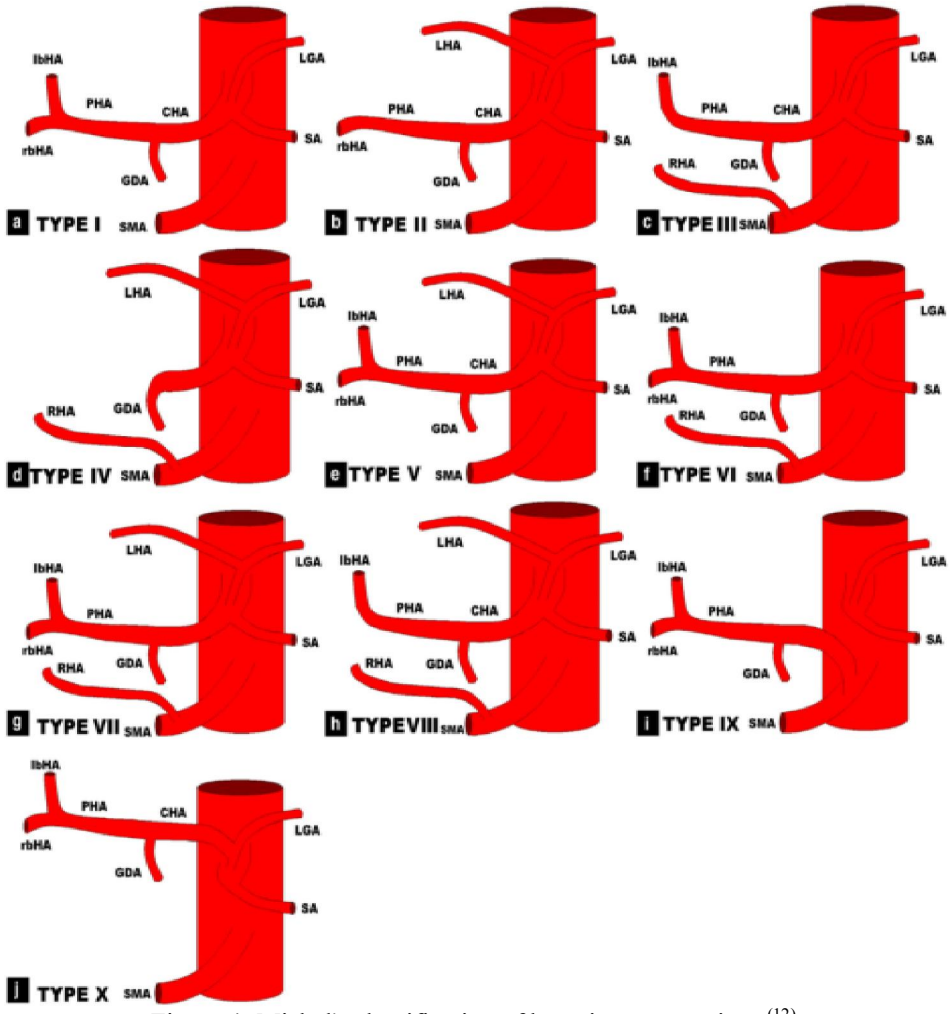

Figure 4: Michel's classification of hepatic artery variants[12].

Table 1: Michel's description of variants of hepatic artery [12].

Type	Description
Type I	Hepatic artery originates from CHA and bifurcates to RHA and LHA.
Type II	replacement of LHA resulting from LGA
Type III	replacement of RHA resulting from LGA
Type IV	replacement of LHA & RHA resulting from LGA
Type V	Accessory LHA resulting from LGA
Type VI	Accessory RHA resulting from LGA
Type VII	Accessory RHA resulting from SMA and accessory LHA resulting from LGA
Type VIII	replacement of RHA and accessory LHA or replacement of LHA and accessory RHA
Type IX	CHA resulting from SMA
Type X	CHA resulting from LGA

2- Portal vein:

The portal vein is the union of the superior mesenteric and splenic superior veins. Upon reaching the liver hilum, the portal vein branches into right and left portal veins. The right portal vein runs to the right, splitting into two branches, providing the right lobe segments of the anterior (V & VIII) and posterior (VI & VII). There is an initial horizontal segment of the left portal vein that at the ligamentumteres (umbilical portion) turns anteriorly. The vertical segment is split from this point into medial (IV) and lateral (Il & Ill) segments of the left lobe [8].

Table 2 & Figure 5 show the most common types of the variations of the portal vein [13].

Table 2: classification of variants of the portal vein [13].

Type	Definition
1	MPV is split into LPV and RPV; then RPV is split into RAPV and RPP
2	MPV trifurcation into LPV, RAPV, RPPV
3	MPV is split into a RPPV and a common trunk, which is then split into LPV and RAPV

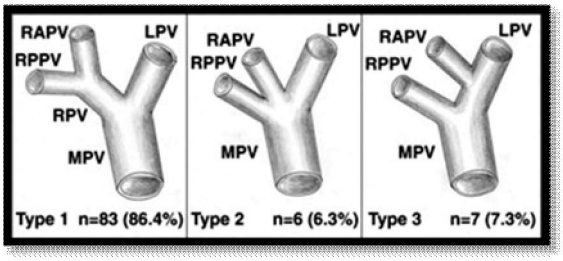

Figure 5: diagram shows the normal variants of portal vein [14].

3- Hepatic veins:

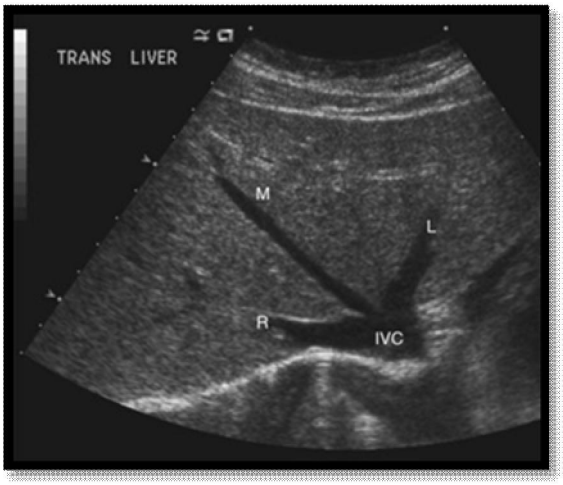

Figure 6: Axial US image of the liver showing normal three hepatic veins and IVC [15].

The venous system of the liver is usually made up three main hepatic veins. The presence of the three W shaped hepatic veins with their base on the inferior vena cava is deemed to be the standard anatomy for these veins. In the vertical fissures separating the liver segments, the three hepatic veins course. They enter the IVC 2 cm caudal to right atrium. Middle and left hepatic veins comprise 60 % of the common trunk. VI-VIII segment is drained into the IVC by the right hepatic vein. The V-IVb segment is drained by the middle hepatic vein, whereas the II-IVa segments are drained by the left hepatic vein. At a lower level, the caudate lobe drains independently via small veins into the IVC. This standard anatomy occurs in 77% of cases (figure6) [15].

C. Biliary system anatomy:

Anatomy of bile duct in the liver follows the segments and portal branches; it exits the liver as a part of the (portal triad) through the hilum. Right and left hepatic ducts drain respectively the right and left hemi-liver, left hepatic duct drains segments II, III, and IV then runs transversely extra-hepatic to join the right hepatic duct. Right hepatic duct drains segment V, VI, VII, and VIII. segment I is drained by multiple ducts joining the right and left ducts [16].

The common bile duct is the common hepatic and cystic duct, it is seen superior and medial to the portal vein, it courses posteriorly to the duodenum and pancreas to join the main pancreatic duct and form the ampulla of Vater (Figure 7).[16]

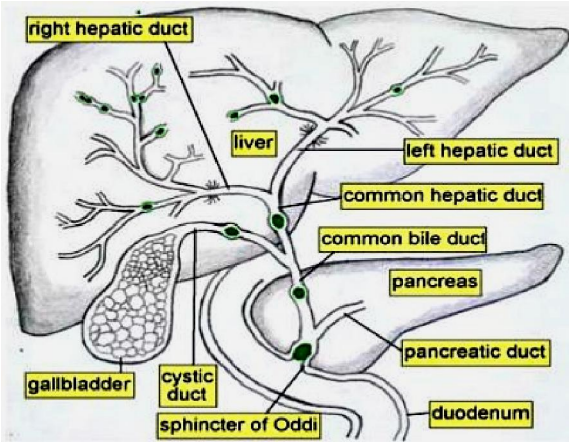

Figure 7: Diagram of the drainage system of the liver, bile and pancreas, also known as the hepato-biliary-pancreatic system [17]

Cirrhosis

It implies damage to the liver tissue. If it is associated with an influx acute or chronic inflammatory cells, this is called hepatitis. Cirrhosis is a process through which progressive (diffuse, fibrosing, nodular) changes affect the entire normal liver architecture [18].

Radiological signs of cirrhosis:

A. Ultrasound (US):

The process of cirrhosis may show up as micronodular, which gives a diffuse coarse echotexture or macronodular (figure 8) in which discrete nodules of 1 cm and above can be seen on US [19]. Superficial nodularity is best detected by high frequency probe [20].

Figure 8: Micronodular cirrhosis by US [19]

1. Liver size:

In the early stage of cirrhosis, the inflammatory process isconsiderable; there is no prominent fibrosis, and so the liver is enlarged in most instances. As the progression of the disease continues, the fibrosingprocess become progressive and the liver volume decreases. The liver is very small at the end stage, which means that fibrosis is remarkable and the liver cells are in rapid regression. In some patients, the cirrhotic liver may not follow the typical pattern within different lobes; the right lobe may shrink, giving rise to relative hypertrophy of caudate and /or left lobes. It is believed to be due to the different venous drainage of the different regions of the liver [21].

2. Liver surface:

At US scanning, the presence of regenerative nodules and fibrous septa is the cause of liver surface nodularity and that is the essential histological findings for diagnosing cirrhosis. It is, therefore, the most accurate sign for cirrhosis. Liver surface nodularity can be a subjective parameter and different variables, primarily local fatty infiltration, may also be affected. For these purposes, numerous scans of the left and right hepatic lobes must be used to evaluate the nodularity of the liver surface. [22]. In case of ascites, irregular and nodular liver surface is more easily assessed and it was observed in 88% of cirrhosis patients [21].

3. Parenchymal echopattern:

The hepatic parenchymal echopatterns were classified as follows:

A. Normal homogeneous pattern.

B. Bright liver pattern, distinguished by the existence of multiple fine, tightly packed echoes of high signal amplitude, uniformly distributed across the liver parenchyma.

C. The existence of non-homogeneous coarse dense uneven echo spots diffusely scattered without any separate hypoechoic nodules reflects the coarse pattern (less than 6mm in diameter) [23].

B. Computed tomography:

The liver can appear normal on cross sectional imaging at an early stage of cirrhosis. The liver parenchyma becomes heterogeneous with disease progression, and surface nodularity is noted, with caudate lobe hypertrophy being the most characteristic morphological characteristic of liver cirrhosis (figure 9). The ratio of transverse caudate lobe width to right lobe width when the value is greater than or equal to 0.65 is an reliable measure for the diagnosis of cirrhosis [24].

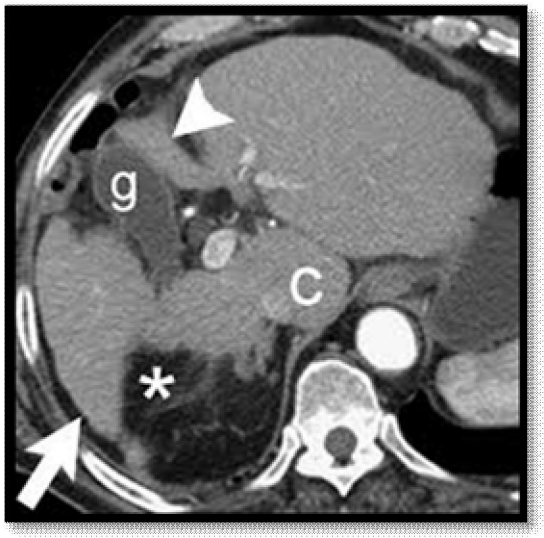

Figure 9: Typical cirrhotic morphology at axial enhanced CT image, showing enlarged caudate lobe (c), enlarged gall bladder fossa (g), medial segment atrophy of the left lobe (arrowhead) and right posterior hepatic lobe (arrow) and right posterior hepatic notch presence (asterisk) [25].

In advanced cirrhosis, other regional changes in hepatic morphology are typically seen, like segmental hypertrophy of the left lobe lateral segments (II & III) and segmental atrophy affecting both the right lobe posterior segments (VI, VII) and the left lobe medial segment (IV) [25].

There are also several irregular strictures associated with the intra and extrahepatic bile ducts. Primary biliary cirrhosis, along with prominent "lacelike fibrosis," regenerative nodules and lymphadenopathy, usually causes early symptoms of portal hypertension as the liver is enlarged. Late-stage primary biliary cirrhosis results in morphological changes that are not distinguishable from other etiologies, such as a shrunken, fibrotic liver[26].

Progressive hepatic fibrosis can cause increased vascular resistance at the hepatic sinusoid level in chronic liver disease. The elevated pressure gradient is referred to as portal hypertension, causing complications such as ascites, leading to the formation of engorged and tortuous collateral vessels that typically form at the lower end of the esophagus (Figure 10) and at the hypertensive gastropathy (gastric fundus). Portosystemic shunts are formed by the reopening of the paraumbilical veins and the left gastric vein. Lienorenal collateral, hemorrhoidal veins, abdominal wall and retroperitoneal collateral are other shunts among the portal and systemic circulation [27].

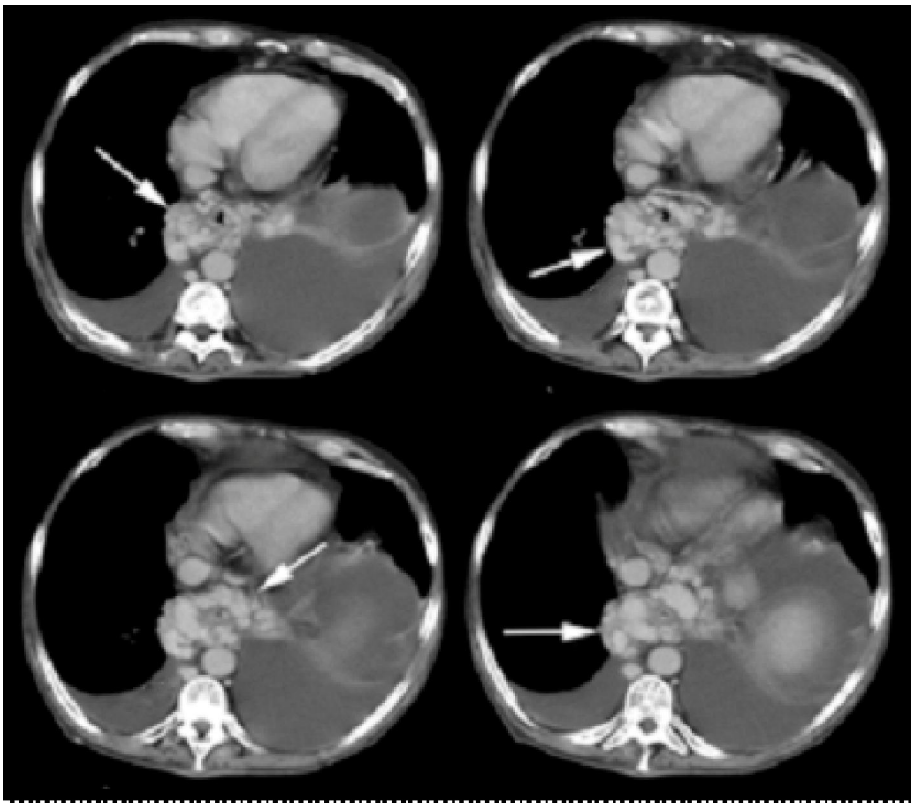

Figure 10: Axial CT images venous phase shows dilated and tortuous esophageal varices (white arrows) [25].

There are many classifications of hepatic focal lesions; pathological classifications depend on whether lesion arise de novo or on top of diseased liver and radiological classification. (Table 3) shows classification of focal liver lesions [28].

Focal liver lesions in cirrhotic liver

HCC is the most popular primary tumor arising in a cirrhotic liver. It represents about 90.3% of the neoplasms located in cirrhotic liver, however, a wide spectrum of benign and malignant lesions other than HCC may be encountered, they represent about 10% showing the following order of frequency: hepatic metastasis (4.2%), cholangiocarcinoma (2.3%), adenoma (l.5%), hemangioma (1.2%) and hematoma (0.8%) [29].

According to the enhancement pattern, liver lesions are split into hypervascular lesions and hypovascular lesions. In conjunction with clinical history, a combination of improvement trends and gross pathological characteristics, such as the existence of fat, blood, calcifications, cystic or fibrotic components, would typically restrict the range the differential diagnosis (table 4) [30].

Table 3: classification of focal hepatic lesions [28]

Benign	Malignant
A-hepatocellular: **1. Hepatocellular adenoma** **2. Focal nodular hyperplasia.** **3. Nodular regenerative hyperplasia** **B-Cholangio-cellular:** **1. Hepatic cyst** **2. Biliary hamartomas** **3. Biloma** **4. Biliary cystadenoma** **C-mesenchymal** **1. Hemangiomas** **2. Hemangioendothelioma** **2-others:** **1. Mesenchymal hamartoma** **2. Focal fat infiltration.** **3. Fatty spared area.** **4. Infectious lesions.** **5. Peliosis hepatitis.** **6. Haematoma** **7. Lipoma.** **8. Myelolipoma** **9. Angiomyolipomas** **9. Leiomyoma**	**A-primary:** 1. hepatocellular: a. Hepatocellular carcinoma. b. Fibrolamellar carcinoma c. Dysplastic nodules d. Hepatoblastoma 2. billiary: a. Biliary cystadenocarcinoma b. Cholangiocarcinoma 3. Others: a. Primary lymphoma. b. Sarcoma **B-Metastatic:** 1. Metastatic carcinoma. 2. Lymphomas.

Table 4: different hepatic focal lesions with different components [30].

	scar	capsule	Calcification	Fat	Blood	Cystic
Hemangioma	+ve		+ve		+ve	
FNH	+ve			+ve		
Adenoma		+ve		+ve	+ve	
HCC	+ve	+ve		+ve	+ve	+ve
Fibrolamellar HCC	+ve		+ve			
Cholangiocarcinoma	+ve		+ve			
Metastasis			+ve		+ve	+ve
Abscess						+ve
Angiosarcoma					+ve	
Cystadenoma		+ve				+ve
Angiomyolipoma			+ve			

A. Hypervascular lesions:

Benign lesions are often arterially improving lesions involving primary liver tumors such as adenoma, FNH, and small hemangiomas which are rapidly packed with contrast. These tumors that are benign need to be distinguished from the most popular hypervascular malignant liver tumors, that include: HCC and hypervascular tumor metastases such as melanoma, carcinoma of the renal cells, breast, sarcoma, and neuroendocrine (islet tumors, carcinoid & pheochromocytoma) [30].

In the arterial phase, hypervascular lesions might look very similar. At the other phases, distinction is accomplished by looking at the improvement pattern and additional gross pathological characteristics along with clinical outcomes. In patients with primary tumors found, hypervascular metastases may be considered. HCC is generally regarded when cirrhosis occurs, whereas FNH is regarded in young females and hepatic adenoma is regarded in patients having anabolic steroids, oral contraceptives or a history of glycogen storage[30].

B. Hypovascular lesions:

There are more common hypovascular liver tumors than hypervascular tumors. Most of the lesions that are hypovascular are malignant and the most frequent are metastases by far. There are exceptions, but primary liver tumors are often hypervascular. 10%

of HCC is hypovascular and cholangiocarcinoma is hypovascularal though it is possible to see delayed improvement (figure 11) [30].

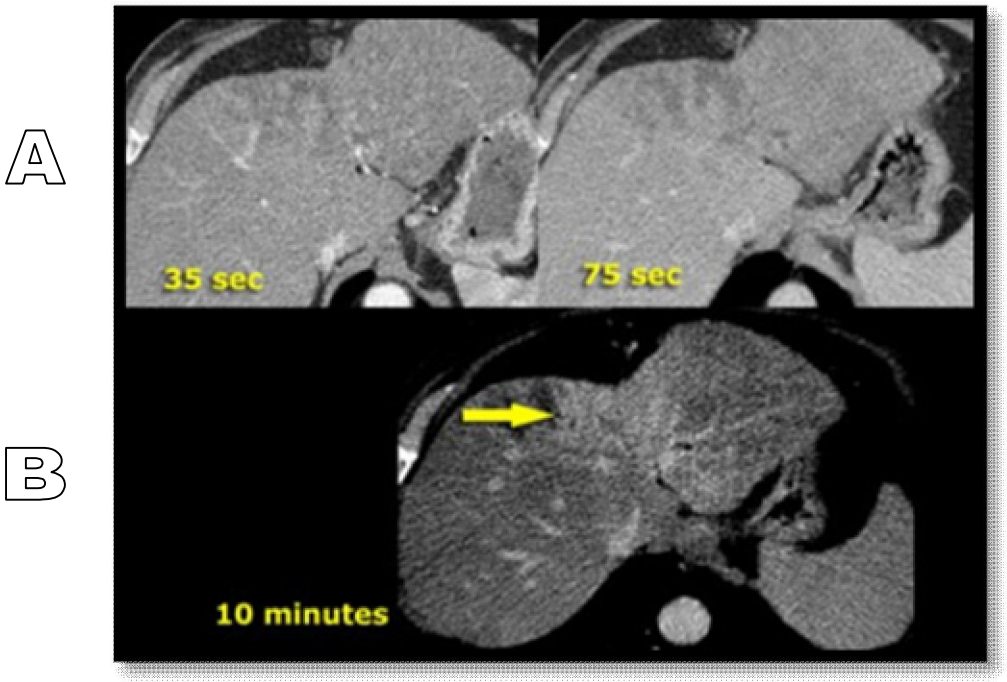

Figure 11: Axial triphasic CT images of the liver show irregularly enhanced hypovascular mass in the late arterial and late portal venous phase (A), a relative dense structure is seen centrally on the delayed images (yellow arrow) that loses its contrast slower than the normal liver. This indicates that the principal component of this tumor is fibrous tissue (B). This fibrous tissue also reacts to the liver capsule. The findings of these images are very suggestive of a cholangiocarcinoma [30]

Hepatocellular carcinoma (HCC):

HCC is a hepatocyte-derived malignant tumor that is part of the main malignant epithelial liver tumor [31]. It is the most common primary hepatic malignancy and one of the world's most visceral malignancies [32]. HCC mostly occurs with cirrhosis of a known cause, such as chronic viral hepatitis B and C or alcoholism [33]

However age-adjusted incidence rates of HCC have doubled in recent decades, and death rates for primary liver cancer have risen more rapidly than for any other leading cause of cancer [34].

Pathogenesis of HCC:

A. Age and gender:

Hepatocellular carcinoma is more frequent in men than in women. This is not due to the fact that men are more susceptible than women to HBV infection. In HCC, the ratio for men and women varies from 2:1 to 5:1. For HCV infection, the corresponding ratio is 1.2:1. There is no knowledge of the origin of this male domination. It takes about 20-30 years for most of the etiological factors of HCC, especially HCV and HBV infections, to result in HCC. The average age of patients with HCC is 65 years in developed countries. Bimodal distribution occurs in developing countries with peaks at 45 and 65 years [35]

B. Risk factors

The pathogenesis of HCC depends on many factors. Environmental, infection, dietary, metabolic and endocrine factors contribute directly or indirectly to hepatocarcinogenesis. HBV, HCV, aflatoxins and alcoholic cirrhosis are the most frequent risk factors for HCC development. The occurrence of the highest frequency HCC found in sub-Saharan Africa and in countries in the Far East where HBV and HCV viruses are endemic[36].

C. Chronic liver disease and HCC

Viruses that affect the liver and replicate in hepatocytes are hepatitis B (HBV) and hepatitis C (HCV) viruses. At birth, most infections happen and more than 90 % are chronic. Nevertheless, only 5-10 % of adults who develop infection adulthood are carriers; and up to 30 % experience progressive chronic liver disease (CLD) that tends to be fibrosis, cirrhosis, hepatitis, and eventually hepatocellular carcinoma. Progression of the disease can arrest at any stage (figure 12)[37].

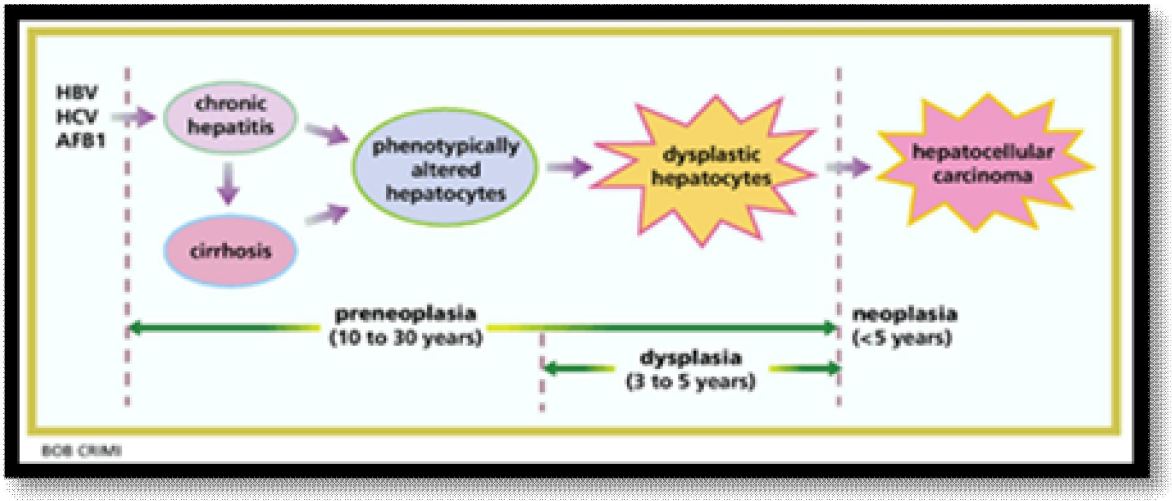

Figure 12: Schematic drawing shows chronologic sequence of cellular lesions culminating in the development of HCC in human [38].

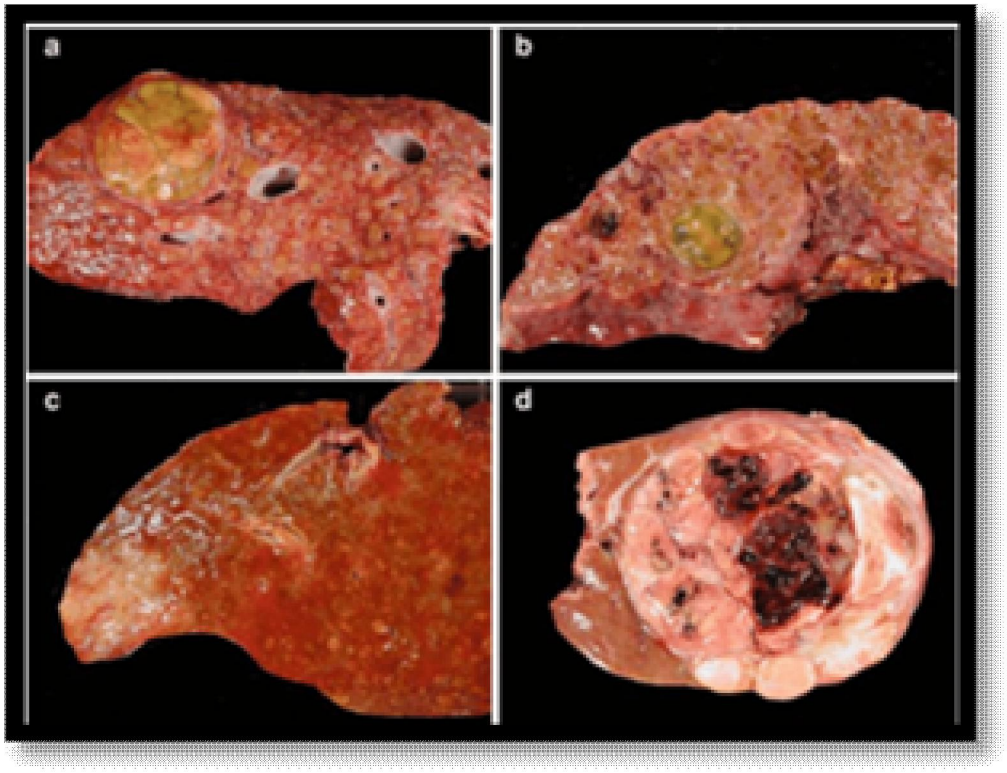

Figure 13: Macroscopic aspects of HCC: (a) Nodular pattern (b) Infiltrative pattern (c) Early HCC on a cirrhotic tissue (d) Nodular HCC developed in a normal liver [43].

The risk of developing HCC between CLD carriers is up to ten- folds relative to uninfected people [39].

Healthy hepatocytes begin to proliferate after liver cell necrosis. Repetitive cycles of necrosis and regeneration characterize chronic hepatitis, promoting successive acquisition of genomic alterations [40].

D. Gross macroscopy of HCC:

HCC usually forms heterogeneous macroscopic masses of soft tissue, polychrome with foci of hemorrhage or necrosis. With a variability in size of less than 1 cm and more than 30 cm, they may be single or multiple. In cirrhosis, the HCC size is

usually smaller relative to those in the non-fibrotic liver [41].

In general, there are three major patterns mentioned (figure 13):

• Nodular pattern:

Throughout the cirrhotic tissue, the most popular nodular (or expanding) pattern is decided by several nodules with one dominant pattern, often partially or totally limited by a fibrous capsule. Metastatic nodules are considered to be small tumor nodules defined as neighboring the main tumor, known as satellite nodules. [42].

Infiltrative pattern:

The infiltrative (or massive) pattern is generally seen in a non-cirrhotic liver and correlated with poor prognosis, comprising of a large, poorly defined single mass with invasive borders [42].

Diffuse pattern:

It is the least frequent pattern which is represented by widespread infiltration of multiple small nodules that mostly replace the entire liver tissue [42].

In macroscopy (macroscopic vascular invasion), affecting portal veins and hepatic veins, HCC vascular invasion can be seen less often and is considered a weak prognostic factor [42].

E. Microscopic picture of HCC:

Hepatocellular carcinoma is a tumor formed of abnormal hepatocytes arranged in a trabecular, sinusoidal pattern in which the trabeculae are separated by sinusoidal blood-filled spaces. Histologically, HCC has been classified by the World Health Organization as trabecular, acinar, compact or scirrhous. Within each type, different grades of tumor are based on the degree of differentiation of the cells. Well-differentiated HCC is a trabecular tumor with a thickness of 2 to 3 cells. There is a typical trabecular pattern of moderately differentiated HCC, while poorly differentiated HCC can have a trabecular, solid or sarcomatous pattern[18].

Triphasic CT appearance of HCC:

Correct assessment of HCC depends mainly on the enhancement pattern. It has been noted that most HCC are hypervascular as a consequence of intratumoralneo angiogenesis, specifically linked to the degree of malignancy of the lesion[44].

Hypervascular lesions show increased enhancement during arterial phase, but during the portal venous phase, Then they become iso or hypodense, that is a sensitive and precise HCC detection pattern [45].

After the introduction of MDCT, By obtaining two arterial phases, one very early [early arterial phase (EAP)] and one immediately following [late arterial phase (LAP)], the passage of contrast material can also be divided. On plain CT images, most HCCs are hypodense when visualized. The EAP image indicates substantial hepatic artery improvement, minimal portal vein improvement, and no hepatic parenchyma improvement. The LAP image has significant improvement of the portal vein, lightparenchymal improvement and no improvement in the hepatic vein. The portal venous phase (PVP) image, on the other hand, there is improvement in the hepatic vein, that's not shown in either EAP or LAP (figure14) [46].

Late arterial phase eases the detection of a greater number of HCC than the EAP does (figure 14). Evaluation of both arterial phases marginally increases sensitivity although there is no statistically substantial difference from LAP alone. EAP is relevant in selected instances of surgery candidates for whom detailed data on vascular anatomy, which can be obtained with 3D reconstruction, is needed. [47].

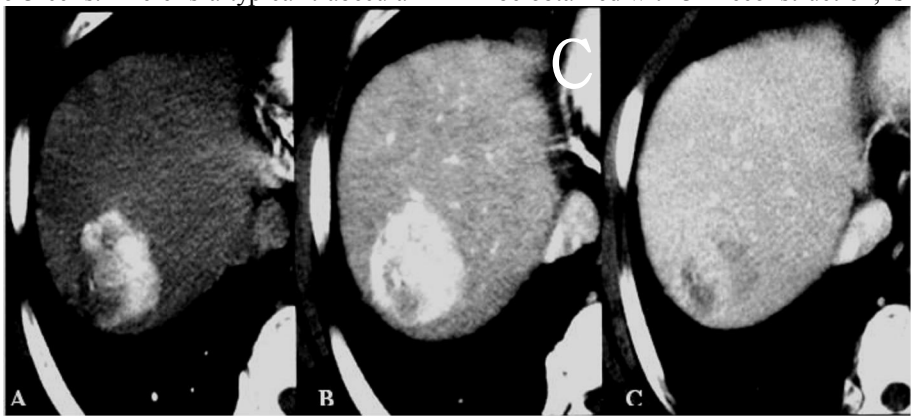

A B C

Figure 14: Axial CT images of the liver show hepatocellular carcinoma which is 35 mm in diameter. (A) Early arterial phase. (B) Late arterial phase. (C) Portal venous phase. Images of the early and late arterial phase and the washout of contrast medium on the image of the portal venous phase, the tumor goes to show marked contrast improvement [47].

The capsule, the connective fibrous tissue at the periphery of the tumour, often surrounds the nodular HCC. The existence of the HCC capsule may mean that within the nodule a tumor is limited. [48].

The capsules appear in CT images as a low-attenuating thin rim that surrounds the nodular HCC on images of the arterial phase and a high-attenuating ring on images of the delayed phase. The capsule may be high or low-attenuating on portal venous phase images.[49].

Arterioportal shunt (APS) may be formed by HCC through invading portal vein and the formation of direct contact among the hepatic artery or its branches and the portal vein. Intrahepatic dissemination and extrahepatic metastasis of carcinoma cells can be accelerated by APS. The gold standard for diagnosis of HCC-associated APS is transcatheter hepatic angiography comprising digital subtraction angiography (DSA), but it has many drawbacks. Due to weak shunting correlated with large HCC, MDCT not only diagnoses APS-revealed DSA, but with DSA, it also lacks mild and peripheral APS. It is a simple, efficient and non-invasive new technique for HCC-associated APS diagnosis (figure 15)[50].

Diagnosis of arterio-portal shunt:

1. Compared with that of the superior mesenteric vein or splenic vein, greater opacification of the main portal trunk and/or first order branches.
2. In comparison with that of the main portal trunk, earlier improvement or greater opacification of the second order and smaller portal venous branches [50].
3. HCC may be diagnosed if a lesion > 2 cm has main HCC characteristics (Arterial phase hypervascularity and portal venous or delayed phase washout) with contrast-enhanced CT or MRI or if these characteristics are shown in both methods by a mass measuring 1-2 cm. The main difficulty in imaging is the characterization of hypervascular nodules < 2cm, which often have nonspecific imaging characteristics and hypovascular nodules [51].

Liver Landmarks By Ct Imaging

The hepatic veins divide the following segments:

The left hepatic vein distinguishes segment II from segment IV; the middle hepatic vein distinguishes segment IV from segments V and VIII and the right hepatic vein distinguishes the anteriorly situated segments V and VIII from the more posteriorly situated segments VI and VII (figure 16) [9].

The right and left veins are the primary portal vein branches. The right portal vein has an anterior branch which sits centrally inside the right lobe's anterior segment and a posterior branch that sits centrally inside the right lobe's posterior segment. The lower segments (V and VI) are caudal to the portal bifurcation and the upper segments (VII and VIII) are cranial to it. Therefore, segment V will be below and segment VIII above in the right anterior sector and segment VI below and segment VII above in the posterior sector [8].

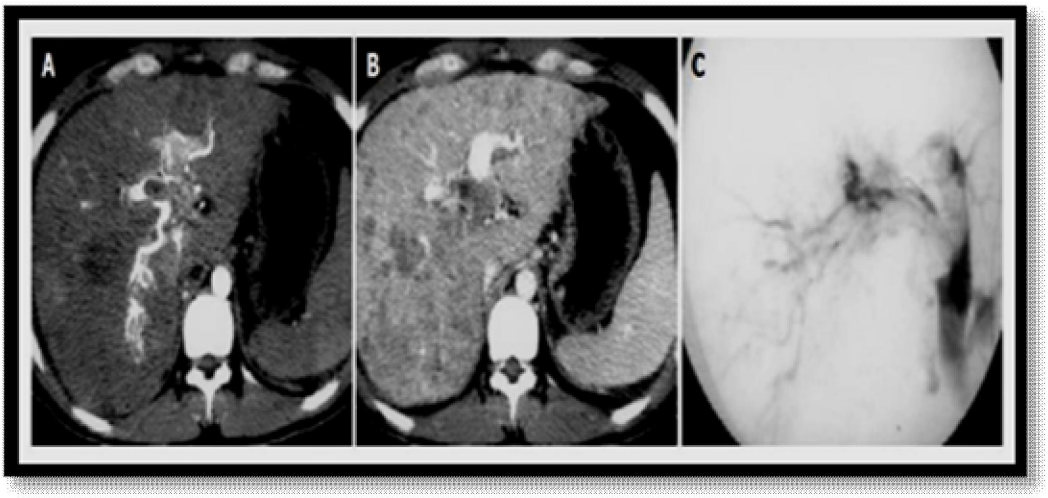

Figure 15: (A & B) axial CT image of the liver show diffuse HCC pattern complicated with extreme and central APS. Earlier improvement and greater opacification of main portal trunk, left and right first-order branches, with thromboses in them; reduced degrees of improvement of HCC foci and spleen. (c) DSA image of the hepatic finding of the same patient (C) [50].

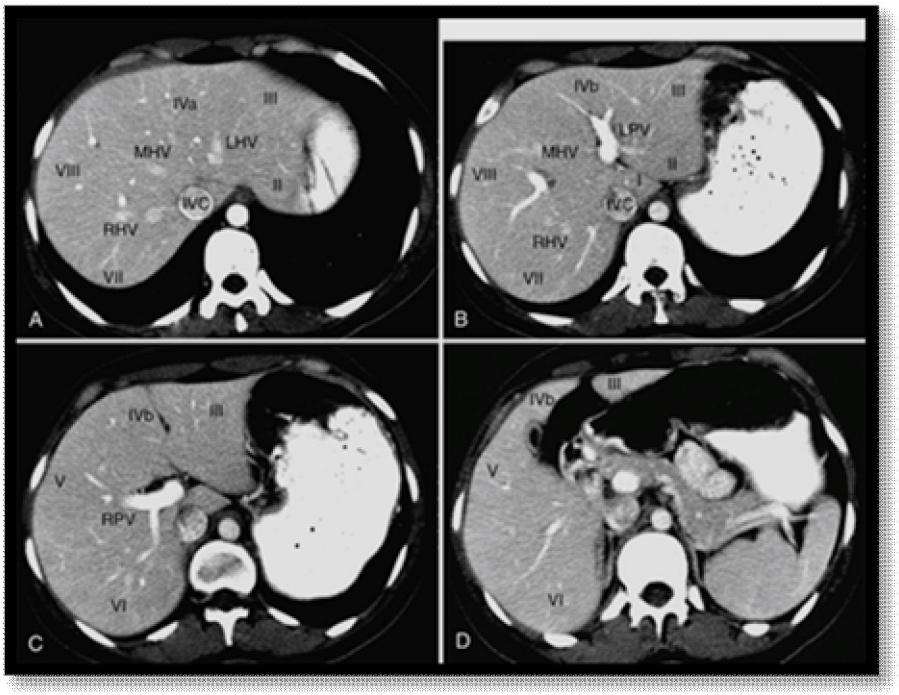

(Figure 16): A through D, Axial contrast-enhanced images of hepatic segments from superior to inferior levels. LHV, Left hepatic vein; LPV, left portal vein; RHV, right hepatic vein; RPV, right portal vein[10].

A smooth arch from the main bifurcation to the round ligament is defined in the left portal vein that runs anterior to the caudate lobe. Segment IV will be all liver tissue comprising of the concavity of the arch and the middle hepatic vein. The distal portion of the left hepatic vein will distinguish segment II (posteriorly and superiorly) from segment III (more anteriorly and inferiorly) at the convexity of the arch on the left side (the left lobe of the descriptive anatomy). So, superior liver segments include segments II, IVa, VIII and VII while inferior liver segments include segments III, IVb, V and VI. Anatomical features, identified by hepatic and portal veins, can be shown on the CT only after contrast media injection. In fact, these vessels are barely visible during the arterial phase on baseline scans and during a liver CT scan. To allocate the correct segment, an accurate match among arterial phase and portal-venous phase images is required, even considering that certain lesions are better represented during the arterial phase[9].

Imaging techniques of focal hepatic lesions

- **Computed Tomography**

A. Specifications of the Examination

Since the invention of MDCT in the late 1990s, liver imaging by CT has progressed impressively. The regular use of thinner, sub-millimeter parts along the Z-axis to have greater spatial resolution, and the reduction in the rotation time of gantry, resulting in a substantially decreased scan time, are two significant advantages of MDCT. For the assessment of hepatic vascular anatomy, biliary system and segmental division of hepatic lesions, off-axis reformations are useful. The distinction among benign and malignant diseases is a valuable aspect of the diagnostic work-up of focal hepatic lesions [52].

Trans-axial photographs from just over the diaphragm dome to the upper portion of the sacroiliac joints with a thickness of 5 mm or less are used in the general CT examination of the abdomen. With 5 mm, the pelvis CT stretches from the iliac crest to just below the ischialtuberosities. Often both the abdomen and the pelvis may be studied together, relying on the clinical indication for study. In some instances, in order to reduce the dose of radiation, it might be necessary to limit the region of exposure and to focus solely on the area or organs of concern. In patients with numerous CT studies and follow-up exams, this is particularly recommended. Coronal, sagittal or other more oblique planes can be built from the source image data in addition to axial images in order to address clinical questions to help in the visualization of diseases or to help in preparing for interventional or surgical procedures [53].

Intraluminal gastrointestinal contrast agent can be used orally, rectally, or through a nasogastric or other tube to provide proper imagery of the gastrointestinal tract, unless clinically contraindicated

or inappropriate for clinical indication. This can be a positive contrast agent, such as water-soluble iodinated solution or diluted barium, a neutral contrast agent, like non-absorbable agent or water, or a negative agent, like carbon dioxide or air [31].

In order to display the visceral organs, intra-abdominal fats and muscles, pulmonary parenchyma at the base of the lung and bone structures, we should have appropriate window width and level settings. However, several CT scanner operations are automated, because these parameters can have an effect on the diagnostic efficiency of CT scanning, a number of technical parameters remain operator-dependent [54].

Improving the CT examination technique needs a supervision physician to make suitable CT protocols depending on thorough analysis of patient history (factors that may raise the probability of negative effects to contrast media) and clinical indications and any related imaging studies, where accessible. The protocol should state the following for each area of interest or indication:

1) The amount and type of gastrointestinal contrast media to be administered, the administration route (oral, rectal, nasogastric or other tube) and the duration of administration.

2) The type, quantity, administration rate and time delay among administration and start of the scan if intravenous contrast material is being used. Bolus monitoring must be used whenever it is indicated to enhance the outcomes.

3) Configuration of the detector.

4) Increase of the table and pitch.

5) The thickness of the slice.

6) Interval of reconstruction.

7) The kernel of reconstruction (algorithm).

8) kVp and mAs per slice or range, for adult or pediatric patients, as needed (minimum and maximum mAs for CT).

9) Index of noise (for multidetector CT).

10) The upper and lower extent of the area of concern to be visualised.

11) PACS (Picture Archiving and Communication System) and MIPS (Medical Image Processing System) protocols for sending images as needed

12) Reconstruction of 3D where needed.

13) The data found in the radiation dose report should be maintained in the radiological record for any CT examination [36].

B. Equipment Specifications

A CT scanner must meet or exceed the following capabilities in order to obtain appropriate clinical CT scans of the abdomen and/or pelvis:

1) Helical acquisition with a pitch of among 1 and 2.

2) Rotation time of the scan

3) Minimum thickness of the slice: <2 mm.

4) Limiting the spatial resolution: >81 p/cm for >32cm display field of view (DFOV) and >101 p/cm for < 24 cm DFOV. For the adverse reactions associated with medications, appropriate emergency equipment and medications must be available[55].

Since the invention of the latest generation of MDCT scanners, a number of new applications have been available. CTA is a non-invasive vascular imaging tool; it provides high quality vascular images. With MDCT, increasing the imaging speed, resolution and improved processing made CTA applicable to a wide range of clinical situations, new rendering techniques scan the entire length of vessels in variable planes and give us good angioscopy images [56].

Multiplanar Reformation (MPR) utilizes the axial sections to form an imaging volume. Opaque surface representation of vessels is provided by the Shaded Surface Display (SSD)[56].

For angiographic displaying of CT information, Maximum Intensity Projection (MIP) has been used. MIP shows the brightest voxel across the image along a line from the eye of the viewer, whereas darker voxels are omitted in front or behind. Compared to SSD, MIP enables precise assessment of the vessel diameter[56].

Volume Rendering Technique is the appropriate approach for 3D processing. The brightness, color, and opacity of the vascular image of the arteries and veins distinguish each voxel within the data collection. VR prevents data loss, enhances vessel definition and decreases vessel-bone interface difficulties by using all voxels within a volume.[57].

Parameters and Technical Principles of Hepatobiliary MDCT exam:

The key parameters are:

- ❖ Parameters of acquisition.
- ❖ Parameters of restoration.
- ❖ Application of contrast media.
- ❖ Different hepatic vascular and parenchymal improvement phases [52].

A. Acquisition parameters

Applying thin collimation is becoming a routine part of MDCT as the number of detector channels increases. Of 16, 32, 64 slice scanners, the minimum section collimation is 0.625 mm (GE, Philips), 0.60 mm (Siemens), or 0.50 mm (Toshiba). Thinner slice collimation also leads to a better ability to identify small hepatic lesions due to increased spatial resolution and decreased partial volume average [58]

B. Reconstruction parameters

Straight or curved MPR, MIP, minimum intensity projection (Min IP) and VR are the most relevant rendering techniques for hepatobiliary

MDCT. Indication for the study defines the type of reconstruction needed. [59].

Compared to axial images alone, there is superior visualization of liver segments and lesions with MPR; however, there was no substantial difference in liver lesion detection by using axial or MPR images. To optimize the image quality of MPR images, increasing the reconstruction thickness to several millimeters is essential. [60].

As this projection indicates the largest attenuation difference among vessels and neighboring tissue, MIP images are also used to evaluate hepatic arteries and the portal vein. Min IP for clearer visualization of the anatomy of the biliary tract and congenital abnormalities [31].

Different opacity values can be used in the VR technique (Figure 17) to view both the surface and the interior of the volume. These images are favored by surgeons as a true 3D view of hepatic vascular anatomy is introduced. In preoperative preparation for hepatic resection, assessment of portal vein patency, generation of liver volume and pre-TIPS placement, VRT is recognized as the most effective rendering technique[52].

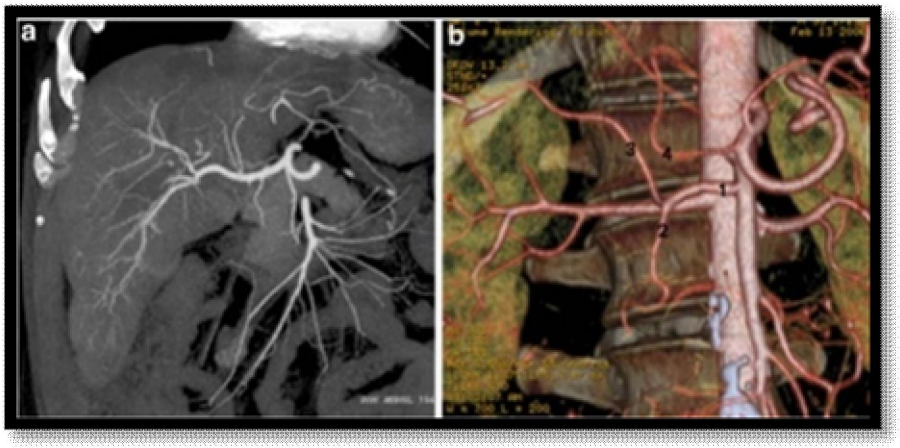

Figure 17: (A) MIP-reconstructed CT angiography of the hepatic artery (B) Volume-rendered CT angiography showing an abnormal origin of the common hepatic artery with the left hepatic artery arising from the celiac axis of the superior mesenteric artery. Legend: l, common hepatic artery; 2, gastroduodenal artery; 3, right hepatic after 4, left hepatic artery [61].

C. Contrast media application:

Tiny extracellular molecular weight agents widely used to identify blood vessels and hepatic parenchyma with hepatobiliary MDCT as well as to identify and describe focal and diffuse hepatic anomalies are non-ionic iodinated contrast agents. The degree to which liver parenchyma is maximally improved during PVP is linked to the amount of iodine administered. Contrast products are available today with an iodine concentration of up to 400 mg / ml. When using an iodine concentration of 300 mg / ml, a fixed amount of contrast agent (120-150 ml) is administered by most institutions. Previous research, however, have suggested that the volume of contrast material should be adjusted to the body weight and the CT scanner i.e low with 128detectors compared with 4 detectors[62].

In MDCT, good injection timing and flow rate must be assessed accurately. The rate of iodine injection and the timing of the contrast bolus mainly affect the hepatic arterial improvement, while the venous phase improvement is calculated by the total dose of iodine given to patients. Compared to 16-row MDCT, the scanning time is further reduced (less than 4 sec for the entire liver) and this involves special modification of the contrast injection protocols, with longer delay times (early and late) of the arterial phases to ensure that the optimal improvement is achieved. Thus, only by accurately timing the scanning delay to the individual circulation time of the patient can different circulatory phases be separated. This is why timing must be calculated by using either a test bolus or an automated computer scanner (bolus tracking) technology[63].

With the exception of patients without circulatory disturbance, a fixed delay time is no longer accepted, because due to inherent variability, such as patient weight and cardiovascular condition, it does not guarantee optimum separation among early and late arterial phases. In the case of bolus monitoring, the region of interest should be set at the celiac axis level and the contrast medium improvement threshold should be set at approximately 150 HU to 180 HU with a delay of approximately 6 sec prior to the beginning the acquisition for the early arterial phase and 20 sec for the late arterial phase. Iodine flux, which relies on flow rate (ml / sec) and contrast

medium concentration (mg of iodine / ml), is the key factor in relation to arterial improvement. Maximum aorta improvement and liver arterial improvement are increased by faster injection rates. It is considered that the optimum flow rate is equal to or greater than 4.0 ml/sec. Intravenous access often limits high infusion rates, and a higher-concentration contrast medium (370 and 400 mg of iodine / ml) is an appropriate alternative)[65].

The entire liver can be screened due to the fast scanning times of 128-row MDCT scanners, in the dead space of the injector tubing, peripheral veins, right heart or pulmonary circulation and central arteries, a significant amount of the injected contrast material resides. Improvement of liver parenchyma is primarily from contrast material supplied via the portal vein; hence, for the purpose of hypovascular liver lesion detection, the contrast material still in the dead space may be deemed lost [65].

D. Different Phases of Hepatic Vascular and Parenchymal Enhancement:

Timing the contrast material bolus is becoming more important because acquisitions are moving closer to a snap shot. Most recently, 64-slice MDCT scanners have imaged the entire liver in less than 2s that can lead to higher hepatic scans in multiple phases with more optimal progress. There are selected cases in which unenhanced liver CT scans are useful and suggested. Appropriate clinical reasons for hepatic CT non-contrast include:

- ❖ Detection of liver acute hemorrhage.
- ❖ Siderotic nodules delineation.
- ❖ Detection and characterization of hepatic calcification (e.g., calcified metastases, hydatid cysts, epithelio idhemangio endothelioma)
- ❖ Assessment of parenchymal liver diseases (e.g., hepatic cirrhosis, hemochromatosis, fatty infiltration).
- ❖ A follow-up CT scan after hypervascular liver lesion embolization [52].

The best single-phase, dual-phase or three-phase CT analysis technique relies on the clinical indication. The multiphasic method suggests that arterial, venous and delayed phase images are accompanied by an unenhanced scan. During the early phase of improvement, images in the arterial phase can be obtained, suitable primarily for CT: angiographic reconstructions and the late phase (arterial dominant phase), beneficial for hypervascular lesion detection [66].

Contrast-enhanced liver MDCT is affected by the dual blood supply of the liver (parenchyma receives 75 % of the blood through the portal vein and 25 % through the hepatic artery), leading in different improvement phases (figure 18). The hepatic artery first improves at about 15s after an intravenous injection of contrast material and achieves peak attenuation at about 30s. The portal vein enhances at approximately 30s after the contrast medium returns from the splanchnic system. Liver parenchyma improvement starts later, hitting a plateau at 60—70s. Eventually, when the volume of contrast material in intra-and extra-vascular space is approximately the same, the Equilibrium Phase (EQP) (3 min and later) occurs[52].

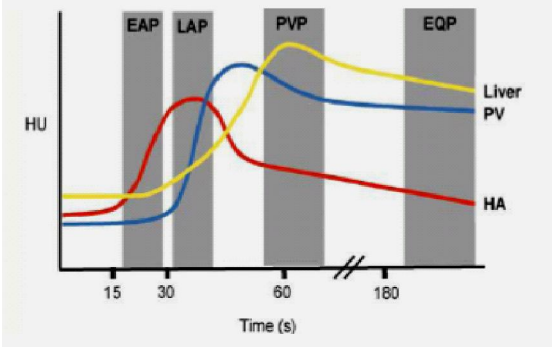

Figure 18: Different dynamic hepatobiliary MDCT imaging enhancement phases (EAP: early arterial phase, LAP: late arterial phase, EQP: equilibrium) [52].

Four phases can be differentiated due to different improvement curves of the hepatic artery, portal vein and hepatic parenchyma:

1) Early arterial phase (EAP) occurs20-25s after administration of the contrast material as the hepatic arteries are clearly enhanced. This phase gives us the least data for liver imaging, as neither hypervascular liver lesions nor liver parenchyma have accumulated contrast media at that time. In spite of that, this phase is well adapted for CT angiography to assess the anatomical structure of hepatic arteries subsequent to liver transplantation and resection of hepatic tumors. An automated trigger system can be used to achieve a high timing of EAP scanning for hepatic CT angiography. An automated trigger system can be used to achieve a high timing of EAP scanning for hepatic CT angiography. The scan for the EAP starts when the trigger that tracks the descending aorta reaches a predefined attenuation (usually 90-100 HU) [52].

2) Following the onset of contrast material administration, late arterial phase (LAP) is reached at around 30-35s. An extra 8 to 10s delay is needed for optimal timing using the automated triggering technique to prevent the EAP. During the LAP, the hepatic arterial systems and prominent neovasculature of hypervascular hepatic neoplasms appear to strengthen although there is only marginal hepatic parenchyma improvement. The optimal phase for the identification of hypervascular liver neoplasms is LAP (Figure 19) [52].

3) After initiation of a contrast media bolus, as the improvement in liver parenchyma hits its peak and the portal veins and hepatic veins are well improved, the portal venous phase (PVP) or hepatic venous phase appears at around 60-70 seconds. The PVP trigger is positioned in the liver parenchyma to monitor the improvement curve for precise timing of a single-phase test and when attenuation reaches the threshold (e.g. 50-70 HU), the table is shifted to the top of the liver, beginning the diagnostic scan. Following the conclusion of the LAP for a dual-phase exam, there is a fixed time delay of 40. During PVP, hypovasculartumors are optimally identified when liver parenchyma improvement is maximal and there is the biggest difference in liver-to-lesion attenuation. PVP is also the appropriate phase for intrahepatic bile duct assessment [52].

4) Equilibrium phase (EQP) or interstitial phase occurs approximately 3 minutes after injection when the diffusion of contrast media into liver parenchyma is increased and the gap in attenuation is minimal among parenchyma and vessels. In various liver lesions, washout of the contrast material can differ according to their histological nature. Intrahepatic cholangiocarcinoma, which displays a delayed washout relative to surrounding liver parenchyma, is one direct indicator of obtaining images during the EQP. By contrast, HCC can exhibit rapid washout compared to the surrounding liver parenchyma during the EQP [67].

Radiation issues:

The radiation dose should also be taken into account to take greatest benefit of the capacity of MDCT (68). The changes in the tube potential (kilovolt) and current (milli-amperes) affect both the exposure to radiation and the quality of the image. The relation among kilovolt and radiation dose is exponential; the impacts on quality of image are complicated, as a decrease in kilo voltage increases image noise, but also enhances the contrast of tissue. A tube capacity of 120 kVp is generally preferred in liver imaging for this reason, reserving 140 kVp for patients who are obese. The relation among the tube current and the dose of radiation is linear; a decrease in mA value increases noise and worsens the resolution of low contrast [61].

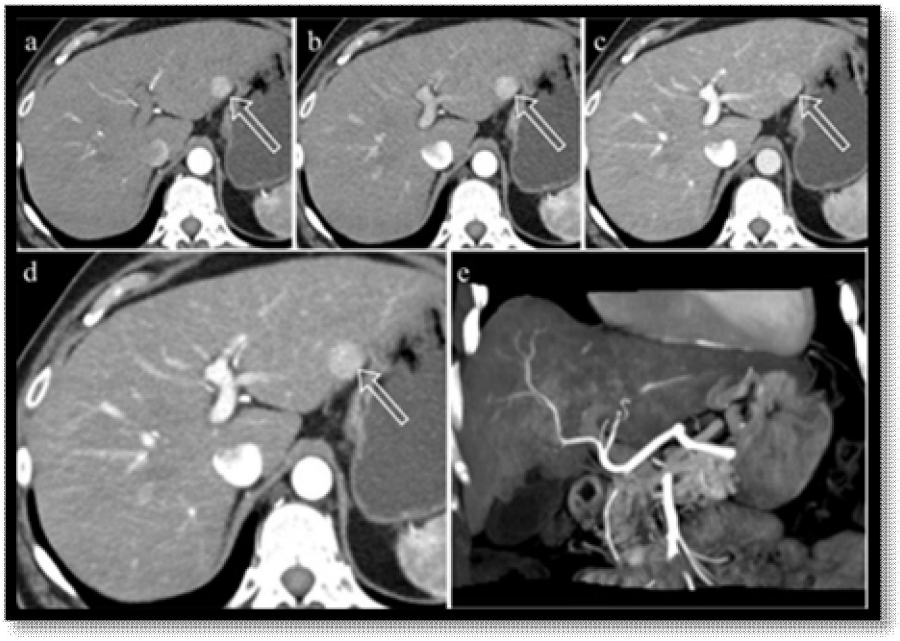

Figure 19: Hyperenhancing or hypervascular liver metastases of the neuroendocrine pancreatic tumor during the LAP [52].

In conclusion:

The ACR standardized system for reporting like hood of HCC (liver imaging reporting and data system) generates high reliability and validity whereas striving to enhance the clarity of imaging reports.

LIRADS sensitivity, specificity, positive and negative predictive values and precision in our research are 92.7%, 100%, 100%, 80.9% and 94.4% respectively.

We found that the importance of LIRADS system is to reduce inconsistencies in the diagnosis of lesions, enhances coordination with physicians, promotes decision-making and management processes, reduces the lack of adequate CT imaging

information by standardizing the content and layout of the study, and enables the monitoring of results, performance auditing, quality assurance and research.

So, we recommend for each hepatic observation to be categorized as regard the LIRADS system and to be reported in radiologist's reports.

Reference

1. Abd Alkhalik Basha M, Abd El Aziz El Sammak D & El Sammak AA (2017): Diagnostic efficacy of the Liver Imaging-Reporting and Data System (LI-RADS) with CT imaging in categorising small nodules (10–20 mm) detected in the cirrhotic liver at screening ultrasound. *Clin. Radiol.* 72, 901.e1-901.e11.
2. Ayuso C, Rimola J & García-Criado Á(2012): Imaging of HCC. *Abdom. Imaging* 37, 215–230.
3. Jang H-J, Kim TK & Burns PN et al., (2007): Enhancement Patterns of Hepatocellular Carcinoma at Contrast-enhanced US: Comparison with Histologic Differentiation. *Radiology* 244, 898–906.
4. An C, Rakhmonova G & Choi J-Y et al., (2016): Liver imaging reporting and data system (LI-RADS) version 2014: understanding and application of the diagnostic algorithm. *Clin. Mol. Hepatol.*
5. Jha RC, Mitchell DG & Weinreb JC et al., (2014):LI-RADS categorization of benign and likely benign findings in patients at risk of hepatocellular carcinoma: A pictorial atlas. *Am. J. Roentgenol.* 203, 48–69.
6. Purysko AS, Remer EM & Coppa CP et al., (2012): LI-RADS: A Case-based Review of the New Categorization of Liver Findings in Patients with End-Stage Liver Disease. *RadioGraphics* 32, 1977–1995.
7. Sutherland F & Harris J (2002): Claude Couinaud: a passion for the liver. *Arch. Surg.* 137, 1305–10.
8. Bismuth H (1982): Surgical anatomy and anatomical surgery of the liver. *World J. Surg.* 6, 3–9.
9. Crocetti L, Della Pina C & Rocchi E et al., (2005): Imaging Landmarks for Segmental Lesion Localization. pp. 63–72.
10. Liver | Clinical Gate. https://clinicalgate.com/liver-3/ (accessed September 2018).
11. Della Pina C, Rocchi E & Conti A et al., (2005): Clinico-Pathological Classification. pp. 203–207.
12. Abdel-Misih SRZ & Bloomston M (2010): Liver anatomy. *Surg. Clin. North Am.* 90, 643–53.
13. Schmidt S, Demartines N & Soler L et al., (2008): Portal Vein Normal Anatomy and Variants: Implication for Liver Surgery and Portal Vein Embolization. *Semin. Intervent. Radiol.* 25, 086–091.
14. Draghi F, Rapaccini GL & Fachinetti C et al., (2007): Ultrasound examination of the liver: Normal vascular anatomy. *J. Ultrasound* 10, 5–11.
15. Hagen-Ansert SL (2017): *Textbook of Diagnostic Sonography : 2-Volume Set*.
16. Castaing D (2008): Surgical anatomy of the biliary tract. *HPB (Oxford).* 10, 72–6.
17. Cholangiopancreatography MRCP. https://www.abdopain.com/magnetic-resonance-cholangiopancreatography.html (accessed March 2019).
18. Heidelbaugh JJ & Bruderly M (2006): Cirrhosis and chronic liver failure: Part I. Diagnosis and evaluation. *Am. Fam. Physician* 74.
19. Lin D-Y, Sheen I-S & Chiu C-T et al., (1993): Ultrasonographic changes of early liver cirrhosis in chronic hepatitis B: A longitudinal study. *J. Clin. Ultrasound* 21, 303–308.
20. Aubé C, Oberti F & Korali N et al., (1999): Ultrasonographic diagnosis of hepatic fibrosis or cirrhosis. *J. Hepatol.* 30, 472–478.
21. Nishiura T, Watanabe H & Ito M et al., (2005): Ultrasound evaluation of the fibrosis stage in chronic liver disease by the simultaneous use of low and high frequency probes. *Br. J. Radiol.* 78, 189–197.
22. Colli A, Fraquelli M & Andreoletti M et al., (2003): Severe Liver Fibrosis or Cirrhosis: Accuracy of US for Detection—Analysis of 300 Cases. *Radiology* 227, 89–94.
23. Caturelli E, Castellano L & Fusilli S et al., (2003): Coarse Nodular US Pattern in Hepatic Cirrhosis: Risk for Hepatocellular Carcinoma. *Radiology* 226, 691–697.
24. Harbin WP, Robert NJ & Ferrucci JT (1980): Diagnosis of cirrhosis based on regional changes in hepatic morphology: a radiological and pathological analysis. *Radiology* 135, 273–283.
25. Brancatelli G, Federle MP & Ambrosini R et al., (2007): Cirrhosis: CT and MR imaging evaluation. *Eur. J. Radiol.* 61, 57–69.
26. Blachar A, Federle MP & Ferris J V. et al., (2002): Radiologists' Performance in the Diagnosis of Liver Tumors with Central Scars by Using Specific CT Criteria. *Radiology* 223, 532–539.
27. Brancatelli G, Midiri M & Lagalla R, et al., (2005) Hepatocellular and Fibrolamellar Carcinoma. In *Focal Liver Lesions*, pp. 209–217.
28. Del Frate C, Zuiani C & Bazzocchi M et al., (2005) Cysts and Cystic-Like Lesions. pp. 85–100.

29. Brancatelli G, Baron RL & Peterson MS et al., (2003): Helical CT Screening for Hepatocellular Carcinoma in Patients with Cirrhosis: Frequency and Causes of False-Positive Interpretation. *Am. J. Roentgenol.* 180, 1007–1014.
30. The Radiology Assistant : Liver - Masses I - Characterisation. http://www.radiologyassistant.nl/en/p446f010d8f420/liver-masses-i-characterisation.html (accessed September 2018).
31. Caoili EM, Paulson EK & Heyneman LE et al., (2000): Helical CT Cholangiography with Three-Dimensional Volume Rendering Using an Oral Biliary Contrast Agent. *Am. J. Roentgenol.* 174, 487–492.
32. El-Serag HB & Rudolph KL (2007): Hepatocellular carcinoma: epidemiology and molecular carcinogenesis. *Gastroenterology* 132, 2557–76. Elsevier.
33. Thompson Coon J, Rogers G & Hewson P et al., (2007): Surveillance of cirrhosis for hepatocellular carcinoma: systematic review and economic analysis. *Health Technol. Assess.* 11, 1–206.
34. Altekruse SF, McGlynn KA & Reichman ME (2009): Hepatocellular carcinoma incidence, mortality, and survival trends in the United States from 1975 to 2005. *J. Clin. Oncol.* 27, 1485–91.
35. Satir AA (2007): An update on the pathogenesis and pathology of hepatocellular carcinoma. *Bahrain Med. Bull.* 29, 64–67.
36. Goshima S, Kanematsu M & Kondo H et al., (2006): MDCT of the Liver and Hypervascular Hepatocellular Carcinomas: Optimizing Scan Delays for Bolus-Tracking Techniques of Hepatic Arterial and Portal Venous Phases. *Am. J. Roentgenol.* 187, W25–W32.
37. Roberts LR & Gores GJ (2005): Hepatocellular Carcinoma: Molecular Pathways and New Therapeutic Targets. *Semin. Liver Dis.* 25, 212–225.
38. Thorgeirsson SS & Grisham JW (2002): Molecular pathogenesis of human hepatocellular carcinoma. *Nat. Genet.* 31, 339–346.
39. Sherman M (2009): Risk of hepatocellular carcinoma in hepatitis B and prevention through treatment. *Cleve. Clin. J. Med.* 76, S6–S9.
40. Röcken C & Carl-McGrath S (2001): Pathology and Pathogenesis of Hepatocellular Carcinoma. *Dig. Dis.*19, 269–278.
41. International Working Party (1995): Terminology of nodular hepatocellular lesions. *Hepatology* 22, 983–93.
42. International Consensus Group for Hepatocellular Neoplasia (2009): Pathologic diagnosis of early hepatocellular carcinoma: A report of the international consensus group for hepatocellular neoplasia. *Hepatology* 49, 658–664.
43. Hytiroglou P, Park YN & Krinsky G et al., (2007): Hepatic Precancerous Lesions and Small Hepatocellular Carcinoma. *Gastroenterol. Clin. North Am.* 36, 867–887.
44. Kim T, Baron RL & Nalesnik MA (2000): Infarcted Regenerative Nodules in Cirrhosis. *Am. J. Roentgenol.* 175, 1121–1125.
45. Murakami T, Kim T & Takahashi S et al., (2002): Hepatocellular carcinoma: multidetector row helical CT. *Abdom. Imaging* 27, 139–146. Springer-Verlag.
46. Murakami T, Kim T & Takamura M et al., (2001): Hypervascular Hepatocellular Carcinoma: Detection with Double Arterial Phase Multi-Detector Row Helical CT. *Radiology* 218, 763–767.
47. Pozzi Mucelli RM, Como G & Del Frate C et al., (2006): TC multidetettore con doppia fase arteriosa e mezzo di contrasto ad elevata concentrazione di iodio nell'identificazione dell'epatocarcinoma. *Radiol. Medica* 111, 181–191.
48. Lim JH & Choi BI (2002): Dysplastic nodules in liver cirrhosis: imaging. *Abdom. Imaging* 27, 117–128.
49. Lee JH, Lee JM & Kim SJ et al., (2012): Enhancement patterns of hepatocellular carcinomas on multiphasicmultidetector row CT: comparison with pathological differentiation. *Br. J. Radiol.* 85, e573-83.
50. Luo M-Y, Shan H & Jiang Z-B et al., (2005): Capability of multidetector CT to diagnose hepatocellular carcinoma-associated arterioportal shunt. *World J. Gastroenterol.* 11, 2666–9.
51. Bruix J, Sherman M & Llovet JM et al., (2001): Clinical management of hepatocellular carcinoma. Conclusions of the Barcelona-2000 EASL conference. European Association for the Study of the Liver. *J. Hepatol.* 35, 421–30.
52. Schindera ST & Nelson RC (2008): Hepatobiliary Imaging by Multidetector Computed Tomography (MDCT). In *MDCTA Pract. Approach*, pp. 49–66.
53. Cohen MD (2009): Pediatric CT Radiation Dose: How Low Can You Go? *Am. J. Roentgenol.* 192, 1292–1303.
54. Flohr TG, Schaller S & Stierstorfer K et al., (2005): Multi–Detector Row CT Systems and Image-Reconstruction Techniques. *Radiology* 235, 756–773.
55. Kanal KM, Stewart BK & Kolokythas O et al., (2007): Impact of Operator-Selected Image

Noise Index and Reconstruction Slice Thickness on Patient Radiation Dose in 64-MDCT. *Am. J. Roentgenol.* 189, 219–225.
56. Indrajit IK, Souza JD & Bedi VS et al., (2005): Impact of Multidetector CT on 3D CT Angiography. *Med. journal, Armed Forces India* 61, 360–3.
57. Francis IR, Cohan RH & McNulty NJ et al., (2003): Multidetector CT of the Liver and Hepatic Neoplasms: Effect of Multiphasic Imaging on Tumor Conspicuity and Vascular Enhancement. *Am. J. Roentgenol.* 180, 1217–1224.
58. Kawata S, Murakami T & Kim T et al., (2002): Multidetector CT: Diagnostic Impact of Slice Thickness on Detection of Hypervascular Hepatocellular Carcinoma. *Am. J. Roentgenol.* 179, 61–66.
59. Hong C, Bruening R & Schoepf UJ et al., (2003) Multiplanar reformat display technique in abdominal multidetector row CT imaging. *Clin. Imaging* 27, 119–23.
60. Jaffe TA, Nelson RC & Johnson GA et al., (2006): Optimization of Multiplanar Reformations from Isotropic Data Sets Acquired with 16–Detector Row Helical CT Scanner. *Radiology* 238, 292–299.
61. Laghi A (2007): Multidetector CT (64 Slices) of the liver: examination techniques. *Eur. Radiol.* 17, 675–683.
62. Ho LM, Nelson RC & Thomas J et al., (2004): Abdominal Aortic Aneurysms at Multi–Detector Row Helical CT: Optimization with Interactive Determination of Scanning Delay and Contrast Medium Dose. *Radiology* 232, 854–859.
63. Brink JA (2003): Contrast optimization and scan timing for single and multidetector-row computed tomography. *J. Comput. Assist. Tomogr.* 27 Suppl 1, S3-8.
64. Itoh S, Ikeda M & Achiwa M et al., (2004): Late-arterial and portal-venous phase imaging of the liver with a multislice CT scanner in patients without circulatory disturbances: automatic bolus tracking or empirical scan delay? *Eur. Radiol.* 14, 1665–73.
65. Fleischmann D (2003): Future prospects in MDCT imaging. *Eur. Radiol.* 13 Suppl 5, M127-8.
66. Foley WD, Mallisee TA & Hohenwalter MD et al., (2000): Multiphase Hepatic CT with a Multirow Detector CT Scanner. *Am. J. Roentgenol.* 175, 679–685.
67. Soyer P, Poccard M & Boudiaf M et al., (2004): Detection of Hypovascular Hepatic Metastases at Triple-Phase Helical CT: Sensitivity of Phases and Comparison with Surgical and Histopathologic Findings. *Radiology* 231, 413–420.
68. Sorrentino P, D'Angelo S & Tarantino L et al., (2009): Contrast-enhanced sonography versus biopsy for the differential diagnosis of thrombosis in hepatocellular carcinoma patients. *World J. Gastroenterol.* 15, 2245–51.

11/14/2020